ANALYSIS OF A PWM-RESONANT DC-TO-DC CONVERTER

Vatché Vorpérian Colonel McLyman

Jet Propulsion Laboratory
California Institute of Technology
Pasadena, California 91109-8099
Tel: (818)-354-9691 Fax: (818)-393-4272

Abstract

When a parallel resonant tank is excited by a bipolar current pulse train a sinusoidal voltage develops across the tank whose amplitude depends on the duty cycle of the pulse train. An isolated secondary can be derived by applying the tank voltage to an isolation transformer whose magnetizing inductance acts as the resonant inductor of the tank circuit. A dc output voltage is obtained after rectification and filtering of the sinusoidal secondary voltage and regulation is achieved by controlling the duty-cycle of the pulse train. The sinusoidal nature of the voltage across the isolation transformer alleviates some of the noise problems associated with parasitic capacitances of an isolation transformer when operated with square voltage waveforms. In this work the dc and small-signal analysis of the converter is given and an equivalent small-signal circuit model is derived. Experimental results which confirm the validity of the model are presented.

Introduction

The converter described and analyzed in this paper has been known to a few designers for many years however it has remained relatively obscure in the general literature and has not been analyzed adequately - specially its small-signal characteristics. The converter operates on a relatively simple principal as shown in Fig. 1. A current pulse train, $\tilde{i}_1(t)$, of adjustable duty cycle is applied to a parallel resonant circuit whose resonant frequency is the same as the frequency of the pulse train. The resonant frequency and the duty cycle shown in Figs. 1a and 1b are defined as follows

$$F_0 = \frac{1}{2\pi\sqrt{L_0 C_0}} \tag{1}$$

$$D = \frac{T_{on}}{T_s/2} \tag{2}$$

The magnitude of the periodic voltage waveform that develops across the tank circuit depends on the duty-cycle of the pulse train. The tank voltage is then rectified and applied to a low-pass filter to yield a dc voltage at its output whose magnitude in turn can be regulated by

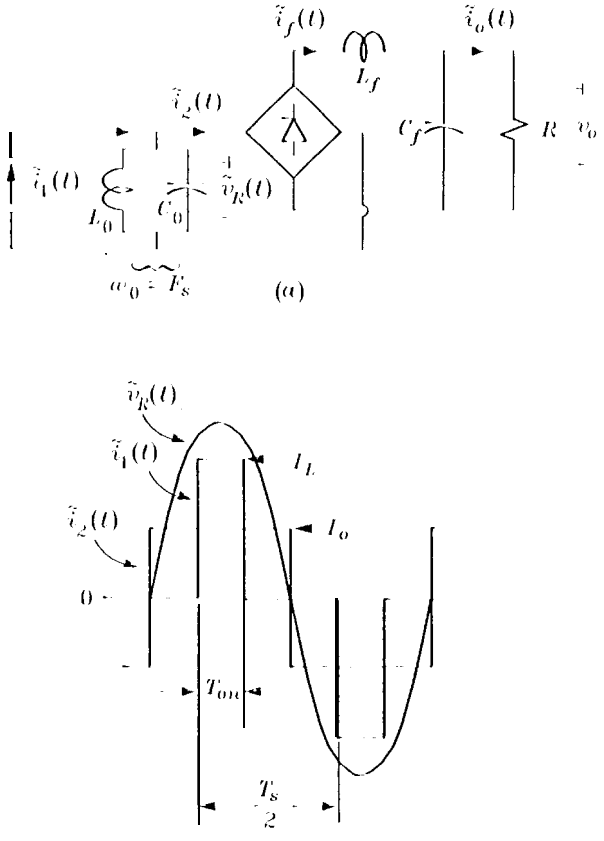

Figure 1 a) The basic principle of operation of the PWM-resonant converter and b) its associated circuit waveforms.

adjusting the duty-cycle of the pulse-train. Practical realizations of the pulsating current source $\tilde{i}_1(t)$ using a feed inductor L with a full-bridge or a half-bridge inverter circuit are shown in Figs. 2a and 2b respectively. The magnetizing inductance of the isolation transformer in these circuits serves as the resonant inductor of the tank

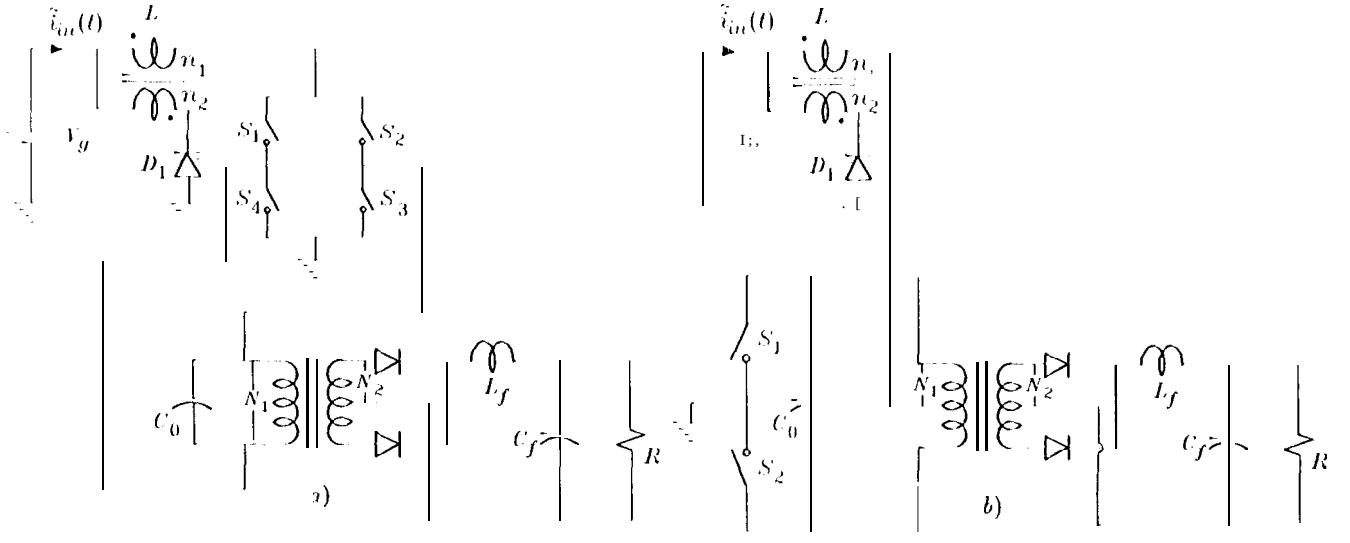

Figure 2 a) Full-Bridge version and b) half bridge version of the PWM-resonant converter.

circuit. The diode D_1 conducts during $T_{on} < t < T_s/2$ when the tank is disconnected from the input feed inductor L in order to reset L. The conversion ratio of this circuit can be easily shown to be independent of the load and given by

$$M = M_I \frac{N_2}{N_1} \tag{3}$$

where M_I is the intrinsic conversion ratio given by

$$M_I = \frac{V_o}{V_g} = \frac{D(1+\pi/2)\sin(\pi/2)}{\sin(\pi D/2)} \tag{4}$$

In order to maintain $M > 0$, the duty-cycle is restricted to the range

$$\frac{1}{n_2/n_1} \leq D \leq 1 \tag{5}$$

Usually, the feed inductor L is wound bi-filar so that $n_1 = n_2$ and the intrinsic conversion ratio is given by:

$$M_I = \frac{V_o}{V_g} = \frac{2D}{\sin(\pi D/2)} \qquad ; \qquad \frac{1}{2} \leq D \leq 1 \tag{6}$$

The primary practical advantage of this converter is that the isolation transformer operates with sinusoidal rather than square voltage waveforms. This is particularly useful in overcoming problems associated with the stray capacitances of an isolation transformer in high voltage and/or low power applications. There are several other topologies that can achieve the same function, notably the forward multi resonant converter [1], but this circuit is considerably simpler, easier to design and better suited for medium switching frequency of operation (< 100kHz).

The following notation is used in this paper:

$\tilde{x}(t)$ = steady-state instantaneous waveform.

$\hat{x}(t)$ = modulated instantaneous waveform.

X = average value of steady-state waveform or DC.

$x = X + \hat{x}$ = modulated average value.

$\hat{x}$ = small-signal modulation in x.

DC Analysis

The circuit in Fig. 1a will be used for dc analysis. It will be assumed that the components are ideal and the output filter inductor L_f and the feed inductor L are large enough that they act as current sources I_o and I_L respectively. We begin by ascertaining the time relationship among the resonant tank voltage $\tilde{V}_R(t)$, the reflected bridge current, $\tilde{I}_2(t)$, and the inverted current pulse train, $\tilde{I}_1(t)$, shown in Fig. 1 1, . The amplitudes of these pulses, I_L and I_o, represent the average current in the feed inductor L (not to be confused with the winding current in n_1 which is discontinuous and the unipolar version of $\tilde{I}_1(t)$, i.e., $|\tilde{I}_1(t)|$ see also explanation for Fig. 5) in the output inductor and the load current, respectively. The periodic voltage waveform across the tank circuit, $\tilde{V}_R(t)$, commutates the rectifier bridge resulting in the current $\tilde{I}_2(t)$ which is in time phase with $\tilde{V}_R(t)$ as shown Fig. 1b. The fundamental component in $\tilde{I}_1(t)$ given by

$$\frac{4}{\pi} I_L \sin \pi D/2 \tag{7}$$

and the fundamental component in $\tilde{I}_2(t)$ given by

$$\frac{4 I_o}{\pi} \tag{8}$$

must be equal and in phase, because the impedance of the tank at the resonant frequency, which is equal to that of the excitation or the fundamental, is infinite. This establishes the relative positions of $\tilde{I}_1(t)$ and $\tilde{I}_2(t)$ in time shown in Fig. 1 b and allows us to determine the average

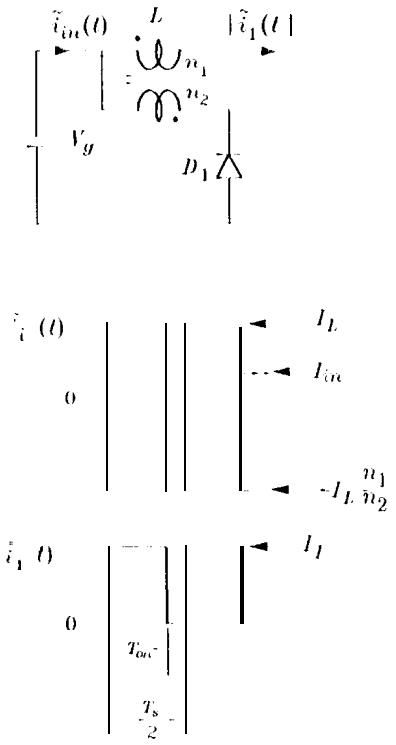

Figure 3 The input feed inductor and its associated waveforms

current gain I_o/I_L by equating Eqs. (7) and (8)

$$\frac{I_o}{I_L} = \sin\pi D/2 \tag{9}$$

The relationship of the average input current to I_L remains to be determined in order to obtain the conversion ratio of the converter. The input current is shown in Fig 3 whence it can be seen that

$$I_{in} = \langle \tilde{I}_{in}(t) \rangle = DI_L - (1-D)I_L n_1/n_2 \tag{10}$$

from which the desired current gain is obtained

$$\frac{I_{in}}{I_L} = D(1+n_1/n_2) - n_1/n_2 \tag{11}$$

The ideal intrinsic conversion ratio follows by substitution of Eq. (11) in Eq. (9)

$$M_I = \frac{I_{in}}{I_o} = \frac{V_o}{V_g} = \frac{D(1+n_1/n_2) - n_1/n_2}{\sin(\pi D/2)} \tag{12}$$

An equivalent circuit for the two-step conversion is shown in Fig. 4. When an isolation transformer is used, the turns-ratio is included as given by Eq. (3).

The average voltages V_L and V_B and the average current, I_L, in L which appear in Fig. 4 require some

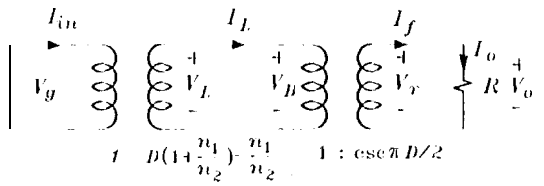

Figure 4 DC equivalent circuit model.

further clarification. Because of the flyback mode of operation of L, the current through it commutates between the two windings n_1 and n_2 and does not flow in a continuous circuit. This makes it hard to visualize the continuous current (flux) in L and its relationship to the circuit in Fig. 4. Likewise the average voltages V_L and V_B in Fig. 4 do not appear in any one place in the original circuit (under dc conditions $V_L = V_B$). These quantities can be physically visualized with the aid of Fig. 5 in which the resetting mechanism has been expanded by the introduction of $V_g n_1/n_2$ and some additional switches. This circuit operates exactly the same way as the original circuit and all the waveforms of the original circuit are seen to be preserved (except for the input current $\tilde{I}_{in}(t)$ which in this case has split between the two sources V_g and $V_g n_1/n_2$.) Furthermore, the continuous current, $\tilde{I}_L(t)$, in L and the voltage $\tilde{V}_L(t)$ can both be seen explicitly. The average value of $\tilde{I}_L(t)$ is given by

$$\langle \tilde{I}_L(t) \rangle = I_L \tag{13}$$

In the forgoing analysis the ripple component of $\tilde{I}_L(t)$ was ignored making the top of the pulse train $\tilde{I}_1(t)$ flat and of amplitude I_L. The average value of $\tilde{V}_L(t)$ in Fig. 5 is given by

$$\begin{aligned} V_L = \langle \tilde{V}_L(t) \rangle &= V_g D - (1-D)V_g n_1/n_2 \\ &= V_g(D(1+n_1/n_2) - n_1/n_2) \end{aligned} \tag{14}$$

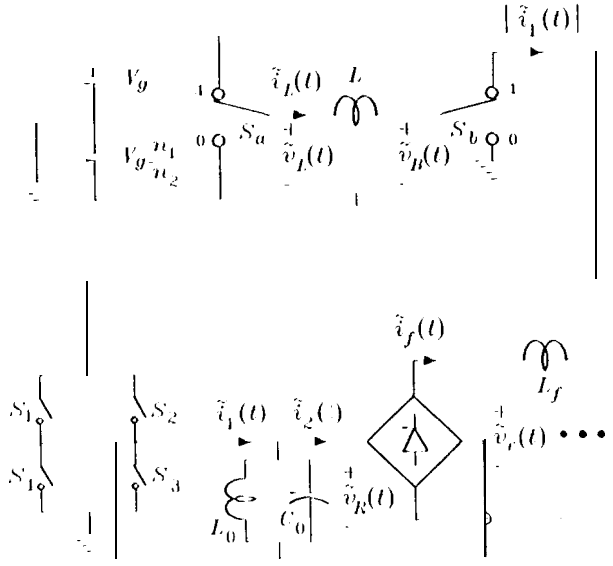

Figure 5 Expansion of the fyback rest mechanism of L. S_a and S_b operate in synchronism and are in the 1 position during T_{on}.

which is consistent with Fig. 4. Hence the "transformer" of turns ratio $1:(D(1+n_1/n_2)-n_1/n_2)$ is an average representation of the nonlinear resetting mechanism which relates the average input current to the average inductor current and the input voltage to the average voltage V_L.

The second transformation, $1:\sec\pi D/2$, in Fig. 4 is an average representation of the inversion and rectification nonlinear mechanisms which relates the average currents I_L and I_f and the average voltages V_B and V_f. In steady state, $I_f = I_o$ and $V_B = V_L$.

Since the tank circuit is excited at resonance, the voltage waveform across it is nearly sinusoidal whose peak value is the peak voltage stress on the switches and the resonant capacitor. This peak can be determined by noting that the average rectified tank voltage is equal to the output voltage which for a rectified sinusoidal waveform is given by

$$V_o = <|\tilde{V}_r(t)|> = <|V_R(t)|> \simeq V_p 2/\pi \qquad (15)$$

Hence, the maximum voltage on the switches and the resonant capacitor is given by (including an isolation transformer)

$$V_{v_{max}} = \frac{\pi}{2}\frac{N_1}{N_2} V_o k_c \qquad (16)$$

in which

$$k_c = \begin{cases} 1 \text{ full bridge} \\ 2 \text{ half-bridge} \end{cases} \qquad (17)$$

The peak current which the switches commutate is approximately I_L (ignoring the ripple in L) the maximum value of which occurs at full load. Hence by Eq. (9)

$$I_{s_{max}} = \frac{I_{o_{max}}}{\sin(\pi D_{min}/2)}\frac{N_2}{N_1} \qquad (18)$$

The critical values of the output and input filter inductors can be shown to be given by (see Appendix)

$$L_{f_{crit}} \simeq \frac{5.26 \times 10^{-2} V_o}{F_s I_{o_{min}}} \qquad (19a)$$

$$L_{1_{crit}} = (N_2/N_1)^2 L_{f_{crit}} \qquad (19b)$$

Small Signal Analysis

The peculiar feature of the small-signal dynamics of this converter is the interaction of the resonant tank with the average quantities which occur in the input and output sides of the converter but not in the resonant tank. From a communication point-of-view, any modulation in the output voltage, input voltage, input current or output current is a base-band information which appears encoded in the envelope of the resonant tank voltage $\tilde{v}_R(t)$ as an AM signal. The interaction of an AM signal with a narrowband filter centered at the carrier frequency has been studied thoroughly in communication circuits [2] and an efficient technique for analyzing this interaction has been devised. The technique presented here is an adaptation of the technique used in communication circuits and has been successfully implemented before in a related circuit described in [3]. Before tackling the problem of the interaction of the resonant voltage with the average quantities, the interaction among the modulated average quantities will be studied first.

The average input current is related to the average inductor current by the input side of the equivalent circuit in Fig. 4 and by the (nonlinear) resetting mechanism given by Eq. (11) which is rewritten here according to the convention in the introduction as

$$i_{in} = i_L(d(1+n_1/n_2) - n_1/n_2) \qquad (20a)$$

Also, according to the equivalent circuit in Fig. 4 the average voltages on both sides of the "transformer" are related by

$$v_L = v_1(d(1+n_1/n_2) - n_1/n_2) \qquad (20b)$$

A small signal perturbation and linearization of Eq. (20a) and (20b) yield

$$\hat{i}_{in} = \hat{i}_L(D(1+n_1/n_2) - n_1/n_2) + I_L(1+n_1/n_2)\hat{d} \qquad (21a)$$

$$\hat{v}_L = \hat{v}_g(D(1+n_1/n_2) - n_1/n_2) + V_g(1+n_1/n_2)\hat{d} \qquad (21b)$$

A circuit equivalent circuit representation of Eqs. (21a) and (21b) is shown in Fig. 6a.

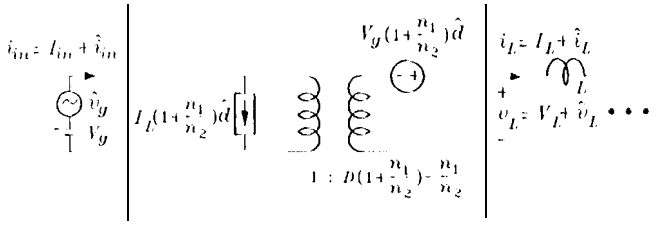

(a)

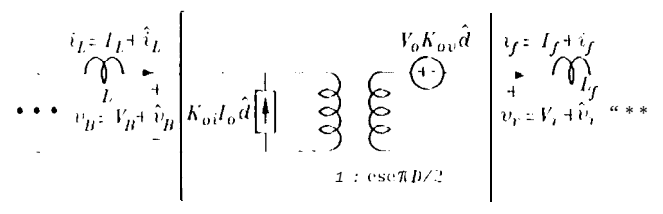

(b)

Figure 6 Small Signal equivalent circuit model of the a) $1:(D(1+n_1/n_2) - n_1/n_2)$ and b) $1:\sec\pi D/2$ transformers in Fig. 4.

The next step is to perturb and linearize the second transformation represented by the 1:$\csc\pi D/2$ "transformer" in Fig. 4. This transformation is an average representation of the inversion and rectification mechanism in the presence of the tank circuit. We have

$$i_L = i_f \csc\pi d/2 \tag{22a}$$

$$v_r = v_B \csc\pi d/2 \tag{22b}$$

A small-signal perturbation and linearization of Eq. (22a) and (22b) yields (note that in steady state $I_f = I_o$)

$$\hat{i}_L = \hat{i}_f \csc\pi D/2 - I_o \frac{\pi}{2} \frac{\cos\pi D/2}{\sin^2\pi D/2} \hat{d} \tag{23a}$$

$$\hat{v}_r = \hat{v}_B \csc\pi D/2 - V_B \frac{\pi}{2} \frac{\cos\pi D/2}{\sin^2\pi D/2} \hat{d} \tag{23b}$$

An equivalent circuit representation of Eqs. (23a) and (23b) is shown in Fig. 6b in which

$$K_{ov} = \frac{\pi}{2} \cot\pi D/2 \tag{23c}$$

$$K_{oi} = \frac{\pi}{2} \cot\pi D/2 \csc\pi D/2 \tag{23d}$$

The interaction of the tank circuit with the average models in Figs. 6a and 6b is determined next. If an arbitrary disturbance in the load current or the input voltage occurs, it will cause the resonant tank voltage to become amplitude modulated which can be written as

$$\tilde{v}_R(t) = (V_p + [\hat{v}]_{env.}(t)) \sin\omega_0 t \tag{24}$$

in which $[\hat{v}]_{env.}(t)$ is the modulation in the envelope of $\tilde{v}_R(t)$ which represents the base-band information in the arbitrary disturbance. Since the modulation in the envelope is essentially given by the peak values, it can now be related to the modulation in the average rectified voltage, v_r, which appears at the input side of the output filter, by a simple extension of Eq. (15)

$$v_r = \frac{2}{\pi} (V_p + [\hat{v}]_{env.}(t)) \tag{25}$$

It follows that the perturbation in the envelope is related to the perturbation in v_r by

$$\hat{v}_r(t) = \frac{2}{\pi} [\hat{v}]_{env.}(t) \tag{26}$$

If the disturbance is a single-tone modulation of frequency ω_m, then the spectra of the various quantities in Eqs. (24), (25) and (26), along with other spectra and the frequency response of the impedance of the tank, are shown in Fig. 7.

The problem we are now faced with is the determination of the response of the impedance of the tank circuit to the modulated waveform $\tilde{v}_R(t)$ from which the perturbations in the average currents i_L and i_f can be deduced. We begin by examining the fundamental components in $\tilde{i}_1(t)$ and $\tilde{i}_2(t)$ which in steady state are equal, as explained in the dc analysis, and are given by

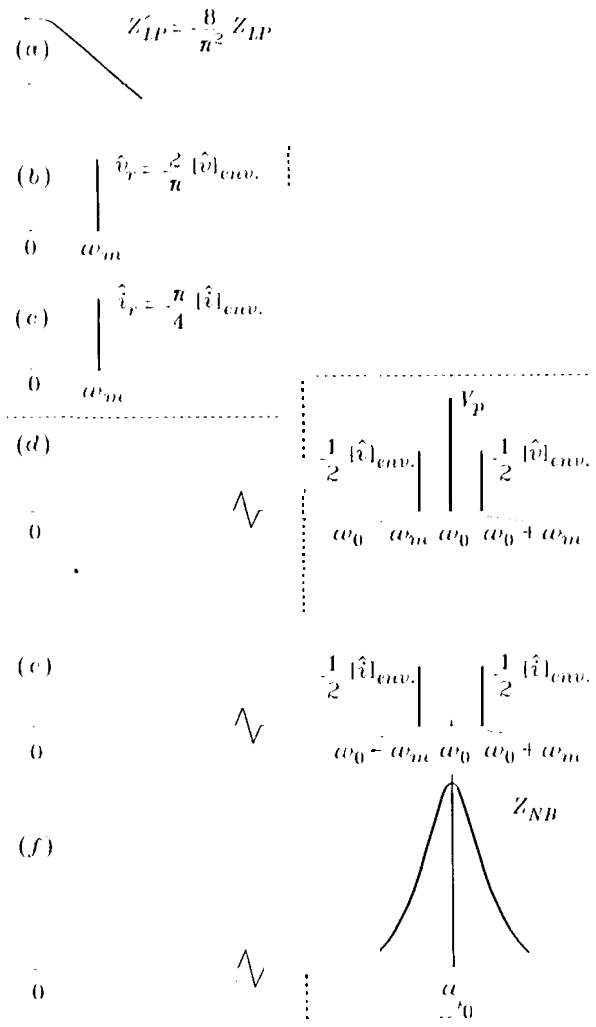

Figure 7 The box on the right shows the interaction of the AM waveform, $\tilde{v}_R(t)$, with the impedance of the resonant filter, Z_{NB}, to produce $\tilde{i}_R(t)$. This problem is solved more easily by studying the interaction of the baseband signals $\hat{v}_r$ and $\hat{i}_r$ with an equivalent low-pass filter Z'_{LP} as shown in the box on the left.

$$\tilde{i}_1^{(1)}(t) = \left(\frac{4I_L}{\pi} \sin\pi D/2\right) \sin\omega_0 t \tag{27a}$$

$$\tilde{i}_2^{(1)}(t) = \left(\frac{4I_o}{\pi}\right) \sin\omega_0 t \tag{27b}$$

A modulation in the average current in the feed inductor and the output filter inductor can be written as

$$i_L = I_L + \hat{i}_L \tag{28a}$$

$$i_f = I_o + \hat{i}_f \tag{28b}$$

The modulated fundamentals in Eqs. (27a) and (27b) are now written as

$$\tilde{i}_1^{(1)}(t) = \left(\frac{4(I_L + \hat{i}_L)}{\pi} \sin\pi D/2\right) \sin\omega_0 t \tag{29a}$$

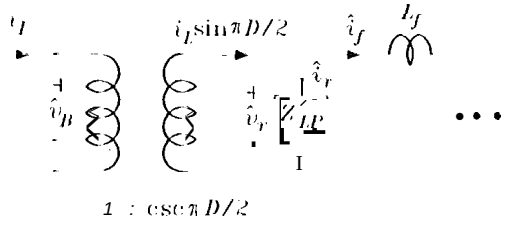

Figure 8 The effective low-pass impedance Z'_{LP}.

$$\tilde{i}_2^{(1)}(t) = \left(\frac{4}{\pi}(I_o + \hat{i}_f)\right) \sin\omega_0 t \qquad \text{(X)1))}$$

The difference between these modulated fundamentals is given by

$$\tilde{i}_R(t) = \frac{4}{\pi}(\hat{i}_L \sin \pi D/2 - \hat{i}_f) \sin\omega_0 t \qquad (30)$$

which can be written in a manner consistent with Eq. (24) as

$$\tilde{i}_R(t) = [\hat{i}]_{env.}(t) \sin\omega_0(t) \qquad (31)$$

in which

$$[\hat{i}]_{env.}(t) = \frac{4}{\pi}\hat{i}_r(t) \qquad (32)$$

and

$$\hat{i}_r = \hat{i}_L \sin \pi D/2 - \hat{i}_f \qquad (33)$$

The modulated current $\tilde{i}_R(t)$ flows through the resonant tank in response to the modulation in $\tilde{v}_R(t)$ in Eq. (24). The spectra of $\tilde{v}_R(t)$ and $\tilde{i}_R(t)$ are shown in Fig. 7 for single tone modulation and are simply connected by the frequency response of the impedance of the resonant tank. Equation (31) represents a DSSC (double sideband suppressed carrier) AM signal which contains the base-band information in the modulation of the average quantities $\hat{i}_L$ and $\hat{i}_f$.

The fact that $\hat{i}_r$ is different from zero suggests that an impedance must be present across the secondary of the $1:\csc\pi D/2$ transformer in Fig. 6b which relates $\hat{i}_r$ to $\hat{v}_r$ by

$$\frac{\hat{v}_r(s)}{\hat{i}_r(s)} = Z'_{LP}(s) \qquad (31)$$

The current $\hat{i}_r$ and the impedance $Z'_{LP}(s)$ associated with it are shown in Fig. 8. Our objective is the determination of $Z'_{LP}(s)$ in order to complete the small-signal equivalent circuit model.

Equations (26) and (32) are the key equations which relate the average quantities of interest to the modulation in the envelope of the resonant tank voltage and current. The envelope of an AM-modulated signal is effected only by the frequency characteristics of the tuned filter in the vicinity of the resonant, or the carrier, frequency. This is so, because the information in the envelope, which is a base-band signal, is encoded or shifted upward near the vicinity of the carrier by the AM process. Furthermore, the spectrum of the information signal in the envelope is only effected by the local behavior of the frequency response of the tank impedance in the vicinity of the carrier frequency. Hence, we seek to determine an equivalent low-pass filter which interacts with the information in the envelope in the base-band region as does the resonant tank with modulated carrier in the vicinity of the carrier. The impedance of this equivalent low-pass filter relates $[\hat{v}]_{env.}(t)$ to $[\hat{i}]_{env.}(t)$ by

$$Z_{LP}(s) = \frac{[\hat{v}]_{env.}(s)}{[\hat{i}]_{env.}(s)} \qquad (35)$$

and is the base-band version of the local behavior of the impedance of the tank in the vicinity of the carrier. According to Eqs. (26), (32), (34) and (35) we have

$$Z'_{LP}(s) = \frac{8}{\pi^2} Z_{LP}(s) \qquad (36)$$

The impedance of the tank is given by

$$Z_{NB}(j\omega) = r_l \frac{(1 + sC_0r_c)(1 + sl_0/r_l)}{1 + sC_0(r_c + r_l) + s^2 l_0 C_0}\Bigg|_{s = j\omega} \qquad (37a)$$

$$= r_l \frac{(1 + j\omega C_0 r_c)(1 + j\omega l_0/r_l)}{1 + j\omega C_0(r_c + r_l) - \omega^2/\omega_0^2} \qquad (37b)$$

where $\omega_0 = 1/\sqrt{l_0 C_0}$ and NB refers to narrow band. Next, the behavior of $Z_{NB}(j\omega)$ near the vicinity of $\omega \simeq \omega_0$ as function of ω is determined by approximating Eq. (37b) as follows. In the denominator we have

$$1 - \frac{\omega^2}{\omega_0^2} = \frac{(\omega_0 - \omega)(\omega_0 + \omega)}{\omega_0^2}\Bigg|_{\omega \simeq \omega_0}$$

$$\simeq \frac{(\omega_0 - \omega)(\omega_0 + \omega)}{\omega_0^2} = \frac{2(\omega_0 - \omega)}{\omega_0} \qquad (38)$$

The two factors in the numerator can be approximated based on the assumption of a high-Q tank as follows

$$1 + j\omega_0 r_c \simeq 1 \qquad (39a)$$

$$1 + j\omega_0 l_0/r_l \simeq j\omega_0 l_0/r_l \qquad (39b)$$

Substitution of these approximations in Eq. (37b) yields the behavior of the impedance of the resonant tank in the vicinity of [d,):

$$Z_{NB}(j\omega) \simeq \frac{r'_c}{1 + j(\omega - \omega_0)C'_c r'_c} \qquad (40)$$

where

$$r'_c = \frac{Z_0^2}{r_c + r_l} \qquad (41a)$$

$$C'_c = 2C_0 \qquad (41b)$$

$$Z_0 = \sqrt{\frac{L_0}{C_0}} \tag{41c}$$

The base-band, or the low-pass, version of Z_{NB} is obtained by a simple downward shift of ω_0 as follows

$$Z_{LP}(j\omega) = Z_{NB}(j(\omega + \omega_0)) = \frac{r'_e}{1 + j\omega C''_e r'_e} \tag{42}$$

It follows from Eq. (36) that

$$Z'_{LP}(j\omega) = \frac{r_e}{1 + j\omega C_e r_e} = r_e \| \frac{1}{j\omega C_e} \tag{43}$$

where

$$r_e = \frac{8}{\pi^2}\frac{Z_0^2}{r_e} + r_l \tag{44a}$$

$$C_e = \frac{\pi^2}{4} C''_e = \frac{\pi^2}{2} C_o \tag{44b}$$

whence it follows that the $Z'_{LP}(j\omega)$ consists of the parallel combination of C_e and r_e. Hence, the final equivalent circuit model is pieced together in Fig. 9. Included in this model is the scaling factor of an isolation transformer which is accounted for by the $1:n$ and $1:k_e$ ideal transformers shown. If the primary of the isolation transformer is center-tapped, as in the case of the half-bridge configuration, then

$$k_e = 2 \quad ; \quad n = \frac{1}{2}\frac{N_2}{N_1} \tag{45a}$$

If the primary of the "isolation" transformer is not center-tapped, as in the case of the full-bridge configuration, then

$$k_e = 1 \quad ; \quad n = \frac{N_2}{N_1} \tag{45b}$$

It does not matter whether the secondary of the isolation transformer is center-tapped or not as long as the turn-ratio is defined as shown in Fig. 10

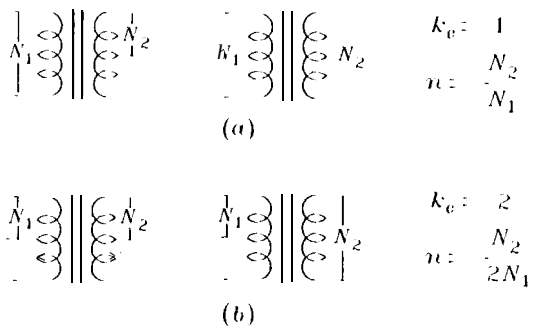

Figure 10 Definitions of n and k_e.

Experimental Results

A half bridge converter was built and the control-to-output transfer function was measured. The agreement between the experimental and predicted results is very good and is shown in Fig. 11. In order to test the model thoroughly, an input filter (L_i and C_i) was added in order to reveal the contribution of the input filter to the transfer function through the "011 (1'01" source $K_{ii} I_L \hat{d}$ on the input side of the circuit model. If a stiff voltage source was used instead, then the control source $K_{ii} I_L \hat{d}$ would have been shorted out and the model would have been verified only partially. The (iii]) that appears in the transfer function is due to the input filter.

The values of the circuit parameters used, in reference to Fig. 9 and starting from the input, are given 1)(1[ )\\. The reset inductor was wound bi-filar ($n_1 = n_2$) so that $f_1(D) = 2D - 1$ and $K_{ii} = 2$.

$V_g = 30 \quad L_i = 1.041\text{mH} \quad r_{L_i} = 2.84\Omega \quad C_i = 20.68\mu\text{F} \quad r_{C_i} = 5\text{m}\Omega$

$2I_1 = .46 \quad 2D - 1 = .88 \quad 2V_g = 60L_1 = .6881[1]1 \quad k_e = 2$

$nI_oK = 9.357 \times 10^{-3} \quad \csc\pi D/2 = 1.0044 \quad \frac{V_oK}{n} = 7.9$

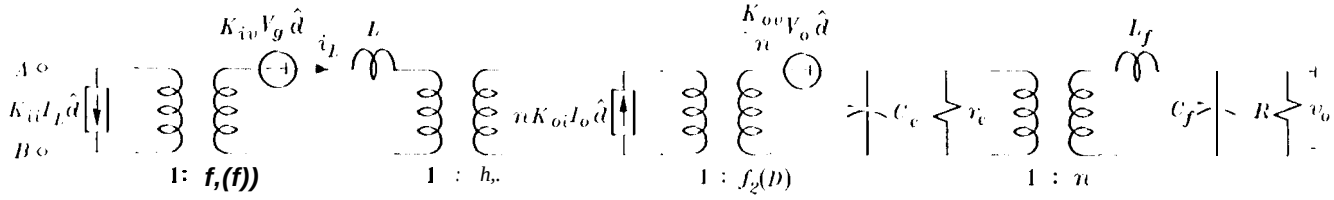

$f_1(D) = D(1 + \frac{n_1}{n_2}) - \frac{n_1}{n_2}$

$K_{ii} = I_L(1 + \frac{n_1}{n_2})$

$K_{iv} = V_g(1 + \frac{n_1}{n_2})$

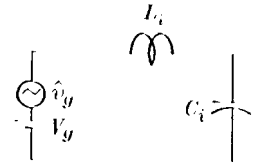

$f_2(D) = \csc\pi D/2$

$K_{oi} = \frac{\pi}{2}\cot\pi D/2 \csc\pi D/2$

$K_{ov} = \frac{\pi}{2}\cot\pi D/2$

Figure 9 Small-Signal equivalent circuit model of the PWM-resonant converter.

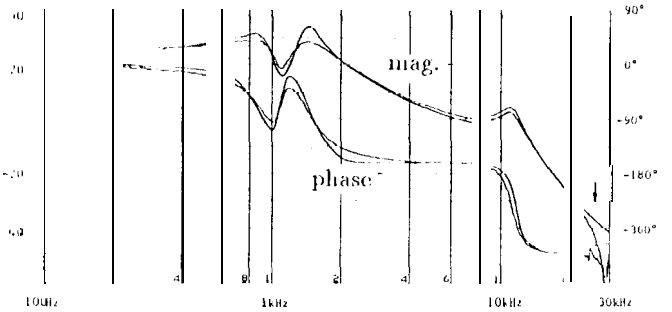

Figure 11 Experimental and predicted results of the control-to output transfer function.

$C_c = .0086\mu F \qquad r_c = 1K\Omega \qquad n = .346$

$r_{L_f} = .76\Omega \quad L_f = 1.45mH \quad r_{C_f} = .95\Omega \quad C_f = 9.83\mu F \quad R_L = 101\Omega$

Appendix

The minimum critical inductance is determined at minimum input line and minimum load conditions at which point it can be assumed that $D \simeq 1$ and $M_L \simeq 1$. Also at this point the voltage waveforms across the input and the output inductors have the same shape and differ only by a factor of N_2/N_1. The voltage waveform across L is shown in Fig. A.1 and is given by

$$\tilde{V}_L(t) = V_g - V_g\frac{\pi}{2}\sin\omega_0 t$$

The shaded area represents the volt-seconds which take the ripple current from a peak to peak. The angle $\omega_0\tau_x$ is given by

$$V_g = V_g\frac{\pi}{2}\sin\omega_0\tau_x \Rightarrow \omega_0\tau_x = .69 \qquad (a.1)$$

The shaded area is given by

$$L(\Delta I_L) = 2\int_0^{\tau_x} V_g(1 - \frac{\pi}{2}\sin\omega_0 t)dt \qquad (a.2)$$

At the critical point $\Delta I_L = 2I_{L,m\_in}$ and Eqs. (a.1) and (a.2) yield the minimum critical inductance in Eqs. (19a) and (19b).

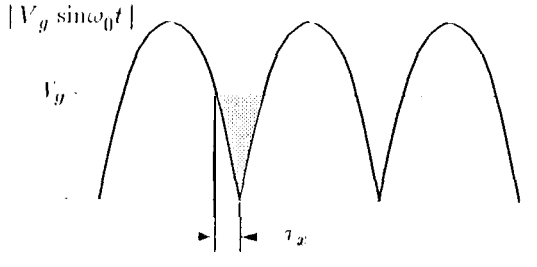

Figure a.1

Acknowledgment

This work was carried out at Jet Propulsion Laboratory, California Institute of Technology, under contract with the National Aeronautics and Space Administration.

References

[1] W.A. Tabisz and F.C. Lee, "A Novel, Zero-Voltage-Switched Multi-Resonant Forward Converter," Proceedings of the High Frequency Power Conference 1988.

[2?] K.K.Clark and 1),'1'. Hess, "Communication Circuits: Analysis and Design," Chapter 3. Addison Wesley.

[3] V. Vorpérian, "A Simple Scheme for Unity Power Rectification for High-Frequency AC Buses," IEEE Transactions in Power Electronics, Vol. 5, No. 1, Jan. 1990, pp. 225-233.